multiphase process comprising three main stages: devolatilisation, gas-phase combustion, and char burnout [65]. When solid fuel particles are exposed to heat, their surface temperature rises, initially causing contained water to evaporate. As the temperature increases further, the solid fuel undergoes thermal decomposition, releasing light gases and tars. This volatile matter mixes with oxygen in the surrounding environment, combusting in the gas phase, a stage that is particularly important for biomass as it involves the rapid release of most energy [35, 65]. In the final stage, the remaining char is oxidised. This chapter addresses gas-phase combustion (second stage) in the form of chemical kinetic models.

In general, solid fuel combustion is a diffusion-controlled process, where the rate of combustion is dictated by the diffusion of oxygen into the flame zone. However, results from direct numerical simulations [29] show that in practical applications, premixed and non-premixed combustion may be relevant due to local extinction and re-ignition. Chemical kinetic models developed for describing oxyfuel combustion must be able to predict such phenomena for the broad range of species observed in volatile matter. At the same time, the high computational cost of simulations, the iterative nature of the model development process, and requirements on uncertainty and richness of experimental data for model validation demand simplifications. The counterflow configuration is the simplest configuration that reflects the importance of both non-premixed combustion and Damköhler numbers. Additionally, its relatively simple geometry permits the analysis of kinetic models through numerically obtained one-dimensional similarity solutions [61], reducing the computational effort. Therefore, this work's validation and analysis of chemical kinetic models focuses on ~~experimental~~ measurements in counterflow diffusion flames. These are complemented by experimental data from jet-stirred reactors (JSRs) covering the premixed combustion modes.

Besides combustion phenomena, such as heat release, extinction, and re-ignition, solid fuel combustion modelling often requires quantifying pollutants, such as nitrogen oxides (NO_x) and soot. Accurate NO_x predictions can be challenging for biomass combustion because of the high content of organically bound nitrogen (N) within the molecular structure of the fuel [55]. The release of nitrogen-containing volatiles leads to potentially high NO_x emissions [23, 26], necessitating the investigation of their formation pathways. Further, prediction uncertainties of soot formation and oxidation remain large and can often exceed two orders of magnitude [39]. Although accumulating evidence suggests that polycyclic aromatic hydrocarbons (PAHs) are the gaseous precursors of soot particles [39], several steps in the formation processes of this pollutant are not yet fully understood and remain an active area of research. This work assesses the progress towards quantitatively accurate predictions of these pollutants under oxyfuel conditions. NO_x and soot formation are relatively slow processes compared to fuel oxidation. Therefore, residence time strongly impacts NO_x and soot formation. The counterflow and JSR configurations facilitate direct access to residence times, which makes it possible to mimic the

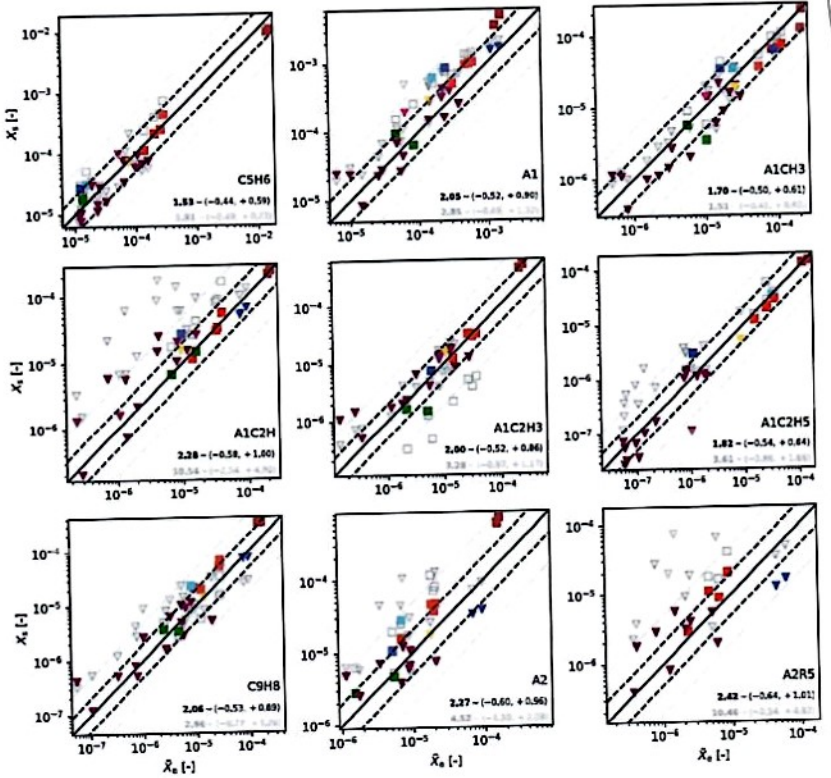

Figure 6.1: Parity diagrams comparing peak mole fractions from ~~experimental~~ measurements to simulation results. Single species or isomer mole fractions were selected as appropriate for the respective experiment. Dashed lines indicate a deviation of a factor of two, and dotted (gray) lines a factor of five. Results obtained with the ITV model [32] use colours representing the fuel composition, green: acetylene [4], purple: ethylene [11, 21], blue: allene or propyne [32, 38], cyan: allene/vinylacetylene [32], magenta: 1,3-butadiene [48], red: 1-butene or 1-butene blends [6], brown: methane-doped cyclopentene [5], gold: *n*-heptane [66]. Results obtained with the model of Cai et al. [10] are shown as empty, (gray) symbols. Experimental data measured as a part of the Transregio 129 Oxyflame project are shown as squares, and other literature data are shown as triangles. Values in the bottom right are the average deviation factor and estimates of the associated 90 %-confidence intervals [39] for the ITV model [32] (black) and the model of Cai et al. [10] ((gray)), respectively.

Symbols too small ↓ reduce number of diagrams to 6 and enlarge those, or plot them like this

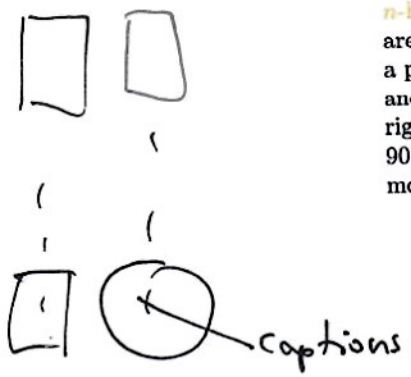

Fonts too small (not smaller than captions!) the grey is unreadable ↳ change!

unreadable!

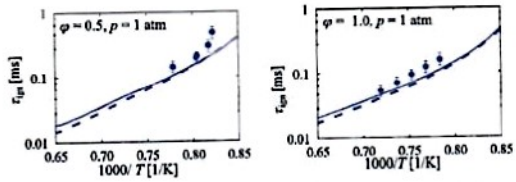

(a) $X_{CO_2} = 0.755$ (b) $X_{CO_2} = 0.720$

Fonts / symbols too small

Figure 6.4: Comparison of ignition delay times of $C_2H_4/O_2/CO_2$ mixtures at lean and stoichiometric condidtions in a shock tube. Symbols denote the measurements [52], solid lines denote model predictions with the ITV-Compact model, and dashed lines denote the ITV model [32] predictions.

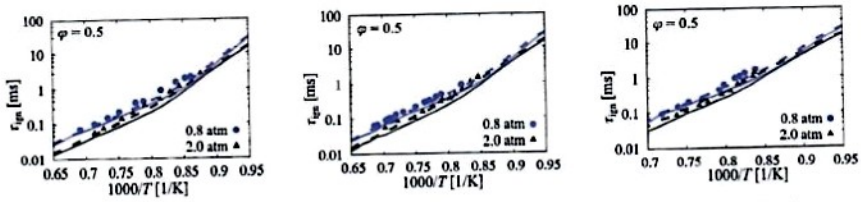

(a) $X_{CO_2} = 0.30$ (b) $X_{CO_2} = 0.60$ (c) $X_{CO_2} = 0.86$

Figure 6.5: Comparison of ethane ignition delay times of lean $C_2H_6/O_2/CO_2$ mixtures in a shock tube. Symbols denote the measurements [43], solid lines denote model predictions with the ITV-Compact model, and dashed lines denote the ITV model [32] predictions.

Anisole chemistry

Figures 6.7 and 6.8 show experimental speciation profiles of major and intermediate species from the counterflow diffusion flame of Chen et al. [13] with CO_2 as a diluent on the oxidiser side (CO_2O-Flame). Additionally, prediction results obtained with the ITV-Based-Anisole, the ITV-Compact model, and the model of Wagnon et al. [62] are presented. The latter was chosen since it provided the anisole-specific chemistry for the ITV-based models. Predictions obtained with the ITV-Compact and the ITV-Based-Anisole models show no discernable difference. Moreover, predictions with the ITV-Based-Anisole and the Wagnon et al. [62] models exhibit no discrepancies, indicating that the differences in their base chemistries ~~impact negligibly.~~ are negligible.

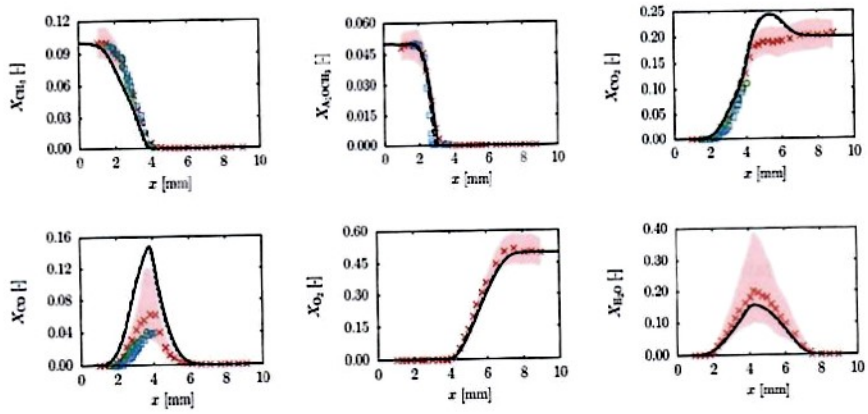

Figure 6.7: Comparison of measured and predicted mole fractions of reactants and main products for the CO_2O-Flame, one of the atmospheric anisole diffusion flames investigated by Chen et al. [13]. Experimental data were obtained using three measurement techniques: ToF-MS (red crosses), GC with an Rt-Q-Bond column (blue squares), and GC with a DB-Petro column (green circles). Predictions with the ITV-Compact model, the ITV-Based-Anisole model, and the model of Wagnon et al. [62] are depicted by solid, dotted, and dashed lines. The red-shaded areas indicate the uncertainty in the ToF-MS measurements. The spatial coordinate x refers to the distance from the fuel nozzle.

predictions with the ITV-Based-NO_x model to assess the impact of differing base chemistries on NO_x formation pathways. This comparison is particularly relevant for cases with potential interactions between nitrogen-containing species and smaller hydrocarbons. Further, the ITV-Based-NO_x model's performance was evaluated against the performance of the model of Glarborg et al. [26], since it is the reference source for C-N chemistry. Flow reactor measurements [25, 26, 33] served as validation targets for the oxidation of hydrogen cyanide (Fig. 6.10) and isocyanic acid (Fig. 6.11). The predictions with the ITV-Compact-NO_x and ITV-Based-NO_x models closely align and show only minor discrepancies compared to those with the model of Glarborg et al. [26]. Matching the latter highlights the successful preservation of the predictive accuracy of the C-N chemistry. Similarly, Fig. 6.12 illustrates good agreement between predictions with the ITV-Compact-NO_x and ITV-Based-NO_x models for NO formation from CH_4/NH_3 oxidation at different fuel-air equivalence ratios. Differences in ammonia consumption compared to the model of Glarborg et al. [26] were attributed to variations in the ammonia chemistry.
The validation of pyridine oxidation in Fig. 6.13 follows the same scheme as for the smaller volatile species, except that the model of Shamooni et al. [60] was considered since it provided the pyridine chemistry. The predictions with the ITV-Compact-NO_x and ITV-Based-NO_x models agree well and differ little from the ones of the model of Shamooni et al. [60], except for the N_2O profiles, for which they show improved prediction accuracy.
For a more comprehensive validation, the reader is referred to the work of Farmand et al. [**Farmand2025submitted**]. Here, conditions relevant to other NO_x formation pathways were also considered.

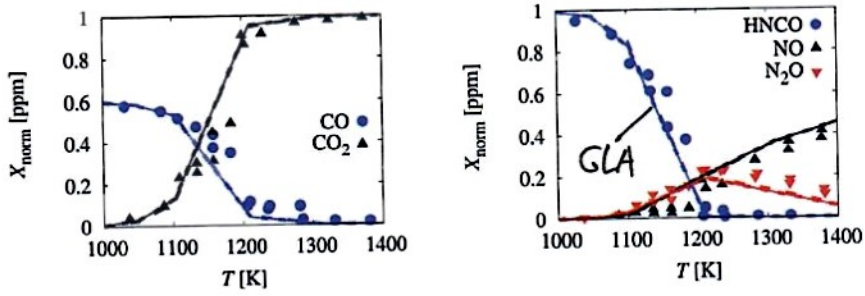

Figure 6.10: Comparison of flow reactor measurements (symbols) of Glarborg et al. [24] for HNCO oxidation at a pressure of 1.05 atm to predictions with the ITV-Compact-NO_x (solid lines), the ITV-Based-NO_x (dotted lines), and the Glarborg et al. [26] (dashed lines) models. The inlet HNCO mole fraction normalizes the shown mole fractions. Inlet mole fractions were HNCO = 480 ppm, CO = 730 ppm, O_2 = 5.5 %, and H_2O = 0.5 %, balanced by nitrogen (N_2).

difference between "dotted" and "dashed" not visible ⇓ indicate ~~models~~ curves by names (see my figure adaptation etc.

(GLA)

6.4 Conclusion

This chapter investigated the gas-phase combustion chemistry of biomass-released volatiles under oxyfuel conditions and in air. Progress in detailed chemical kinetic modelling of PAH formation from combustion under these conditions was evaluated by comparing predictions of two literature models [10, 32]. Both models [10, 32] proved suitable for the investigation of combustion under oxyfuel conditions. However, analyses revealed that the ITV model [32] published in 2024 predicts the mole fractions of aromatic species measured in counterflow flames more accurately than its predecessor published in 2019 [10]. Mean deviations between measured and predicted peak mole fractions of aromatic species obtained with the ITV model [32] are, on average, close to a factor of two for a broad range of conditions and fuels. The enhanced predictive capabilities and revisions of the C_0–C_4 chemistry make the ITV model [32] the recommended choice for further investigations of oxyfuel combustion.
Building upon the ITV model [32], we developed a skeletal kinetic model for biomass combustion. First, a particle devolatilisation model [18, 57] identified the main volatile species released under conditions representative of practical applications to determine a surrogate formulation. Anisole, levoglucosan, and propionaldehyde emerged as representative biomass surrogate components. The chemistry of these volatiles was incorporated from literature kinetic models into the ITV model [32], yielding three detailed models, one for each component. These models were then reduced to a skeletal level and merged to develop a compact surrogate model with 104 species. To account for nitrogen-containing species released from the volatile mixture, we developed a 36-species skeletal NO_x submodel that combines subset models from different literature works. This submodel accurately captures key NO_x formation pathways and the oxidation of small nitrogen-containing volatiles and tars. All developed models were validated against detailed kinetic models and experimental data, demonstrating their reliability in predicting critical aspects of biomass combustion under conditions relevant to practical applications. The developed NOx submodel and a further reduced version of the ITV-Compact model were successfully applied in the numerical simulations conducted in Chap. 19 and Chap. ??, demonstrating their prediction accuracy and suitability for large-scale simulations due to their compact size.

Pielsticker to check